

POINT CLOUD DENOISING VIA MOMENTUM ASCENT IN GRADIENT FIELDS

Yaping Zhao^{1,*}, Haitian Zheng^{2,*}, Zhongrui Wang¹, Jiebo Luo², Edmund Y. Lam^{1,†}

¹ The University of Hong Kong ² University of Rochester

*equal contribution †corresponding author

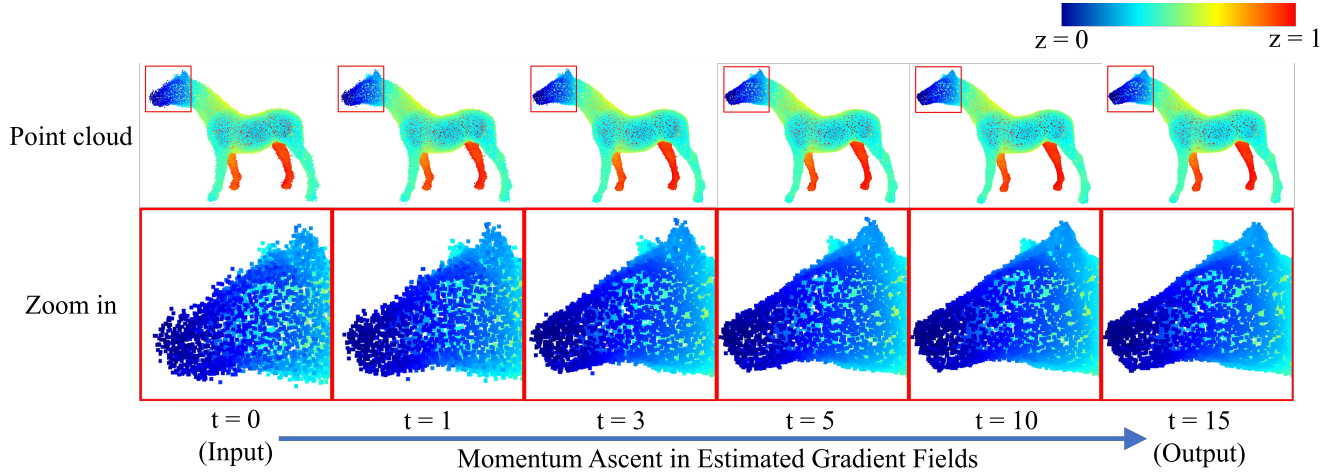


Fig. 1: Given a noisy point cloud as input, we utilize a neural network to estimate the implicit gradient fields, and iteratively update the position of each point by momentum gradient ascent towards the underlying surface. The color of each 3D point varies according to its z coordinate (perpendicular to the plane).

ABSTRACT

To achieve point cloud denoising, traditional methods heavily rely on geometric priors, and most learning-based approaches suffer from outliers and loss of details. Recently, the gradient-based method was proposed to estimate the gradient fields from the noisy point clouds using neural networks, and refine the position of each point according to the estimated gradient. However, the predicted gradient could fluctuate, leading to perturbed and unstable solutions, as well as a large inference time. To address these issues, we develop the momentum gradient ascent method that leverages the information of previous iterations in determining the trajectories of the points, thus improving the stability of the solution and reducing the inference time. Experiments demonstrate that the proposed method outperforms state-of-the-art methods with a variety of point clouds and noise levels.

Index Terms— point cloud denoising, point cloud processing, 3D vision

1. INTRODUCTION

Point cloud denoising aims to restore clean point clouds from noise corrupted ones. Due to the inherent limitations of ac-

quisition devices or matching ambiguities in the 3D reconstruction, noise inevitably degrades the quality of scanned or reconstructed point clouds, for which point cloud denoising is favored. Moreover, the quality of point clouds affects the performance of downstream 3D vision tasks, *e.g.*, detection and segmentation. Therefore, point cloud denoising offers a crucial preprocessing for relevant 3D vision applications.

Unlike image and video denoising, point cloud denoising is challenging because of the intrinsic unordered characteristic of point clouds. Point clouds consist of discrete 3D points irregularly sampled from continuous surfaces. Perturbed by noise, the 3D points can deviate from their original positions and yield the wrong coordinates.

To tackle this issue, traditional methods [1, 2, 3, 4, 5, 6] heavily rely on geometric priors but show limited performance. Deep learning ones [7, 8, 9, 10] denoise by estimating the deviation of noisy points from the clean surface, but often results in outliers due to the coarse one-step estimation. Recently, Score [11] is proposed to iteratively update the point positions according to the estimated gradient fields. However, the predicted gradients can fluctuate, leading to perturbed and unstable solutions, as well as a large inference time.

To improve the performance and efficiency of the gradient-based method, as Figure 1 shows, we propose a novel iterative

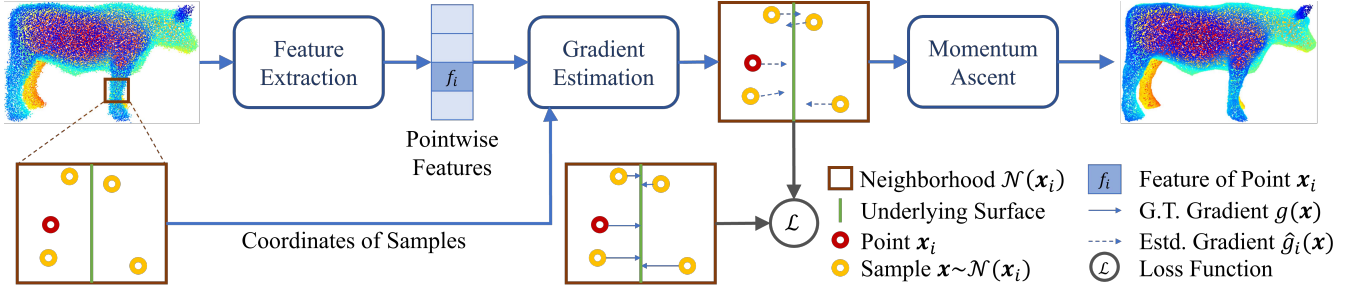


Fig. 2: Illustration of the proposed network architecture.

paradigm of point cloud denoising motivated by the classical momentum method [12] in convex optimization. Specifically, we employ Score [11] to estimate the gradient fields from the noisy point clouds, and compute the displacement of each point according to the estimated gradient. To avoid the fluctuated gradient of Score, we apply a momentum gradient ascent method that utilizes the previous iterations to seek promising directions to move forward, thus improving the solution stability and inference time. Experiments demonstrate that the proposed method outperforms state-of-the-art methods with a variety of point clouds and noise levels.

2. RELATED WORK

To perform point cloud denoising, traditional methods [1, 2, 3, 4, 5, 6] heavily rely on geometric priors but show limited performance. Deep learning-based approaches break the performance limit of the point cloud denoising. Among them, some [7, 8, 9, 10] predict the deviation of noisy points from the underlying surface and reinstate noisy points by reversing the deviation. Unfortunately, the inaccurate estimation of the one-step deviation often incurs outliers. Others [13] predict the underlying manifold of a noisy point cloud for reconstruction in a downsample-upsample framework, which loses details in the downsampling stage.

Recently, Score [11] is proposed to tackle the aforementioned issues by iteratively updating the point position in implicit gradient fields learned by neural networks. However, the predicted gradients suffer fluctuation, leading to perturbed and unstable solutions, as well as a large inference time.

3. METHOD

3.1. Overview

Given a noisy point cloud $\mathbf{X} = \{\mathbf{x}_i\}_{i=1}^N$ consisting of N points as input, we assume the underlying clean point cloud is sampled from a distribution p , and the noise follows a distribution n . Then the distribution of the noisy point can be modeled as the convolution between p and n , denoted as $p * n$. It is worth noting that the mode of $p * n$ is the underlying clean

surface, having a higher probability than its ambient space.

Therefore, we estimate the gradient of the log-probability function, *i.e.*, $\nabla_{\mathbf{x}} \log[(p * n)(\mathbf{x})]$, from \mathbf{X} using a neural network. Then, we denoise \mathbf{X} via momentum gradient ascent, thus moving noisy points towards the mode of the distribution that corresponds to the underlying clean surface. As Figure 2 shows, the proposed method mainly consists of:

1. **Neural Network Architecture.** In Section 3.2, we implement a network that takes noisy point clouds as input and outputs point-wise gradients.
2. **Loss Function.** In Section 3.3, we design the loss term for training the gradient estimation network.
3. **Momentum Ascent Denoising Algorithm.** In Section 3.4, we utilize the estimated gradients to denoise point clouds by momentum ascent.

3.2. Neural Network Architecture

Given a noisy point cloud $\mathbf{X} = \{\mathbf{x}\}_{i=1}^N$ as input, the neural network predicts gradient $\nabla_{\mathbf{x}} \log[(p * n)(\mathbf{x})]$ for each point in \mathbf{X} . The network aims at estimating the gradient in the neighborhood space around x_i , denoted as $\hat{g}_i(\mathbf{x})$. We follow the same network reported in Score [11], which consists of a feature extraction module and a gradient estimation module.

Specifically, the feature extraction module learns point-wise features from the input noisy point cloud \mathbf{X} and the learned feature for point x_i is denoted as f_i . The gradient estimation module takes point coordinates $\mathbf{x} \in \mathbb{R}^3$ surrounding x_i as inputs and outputs the estimated gradient $\hat{g}_i(\mathbf{x})$:

$$\hat{g}_i(\mathbf{x}) = G(\mathbf{x} - \mathbf{x}_i, f_i), \quad (1)$$

where $G(\cdot)$ is the gradient estimation network implemented by a multi-layer perceptron (MLP).

3.3. Loss Function

We denote the ground truth clean point cloud as $\mathbf{Y} = \{\mathbf{y}_i\}_{i=1}^N$, and define the gradient for point \mathbf{x} as

$$g(\mathbf{x}) = N(\mathbf{x}, \mathbf{Y}) - \mathbf{x}, \quad \mathbf{x} \in \mathbb{R}^3, \quad (2)$$

# Points Noise Metric	10K (Sparse)						50K (Dense)					
	1%		2%		3%		1%		2%		3%	
	CD	P2M										
Bilateral [14]	3.646	1.342	5.007	2.018	6.998	3.557	0.877	0.234	2.376	1.389	6.304	4.730
PCNet [10]	3.515	1.148	7.467	3.965	13.067	8.737	1.049	0.346	1.447	0.608	2.289	1.285
DMR [13]	4.482	1.722	4.982	2.115	5.892	2.846	1.162	0.469	1.566	0.800	2.432	1.528
Score [11]	2.521	0.463	3.686	1.074	4.708	1.942	0.716	0.150	1.288	0.566	1.928	1.041
Ours	2.498	0.459	3.629	1.054	4.686	1.923	0.706	0.146	1.287	0.557	1.931	1.045

Table 1: Point cloud denoising comparisons on the PU-Net dataset [15]. CD and P2M are multiplied by 10^4 .

where $N(\mathbf{x}, \mathbf{Y})$ is the point nearest to \mathbf{x} in \mathbf{Y} , $g(\mathbf{x})$ is a vector from \mathbf{x} to the clean surface. Then the loss function is

$$\mathcal{L}_i = \mathbb{E}_{\mathbf{x} \sim \mathcal{N}(\mathbf{x}_i)} [\|g(\mathbf{x}) - \hat{g}_i(\mathbf{x})\|_2^2], \quad (3)$$

$$\mathcal{L} = \frac{1}{N} \sum_{i=1}^N \mathcal{L}_i, \quad (4)$$

where $\mathcal{N}(\mathbf{x}_i)$ is a distribution concentrated in the neighborhood of \mathbf{x}_i in \mathbb{R}^3 space.

3.4. Momentum Ascent Denoising Algorithm

Though we can directly use $\hat{g}_i(\mathbf{x})$ to move \mathbf{x}_i , we use the ensemble gradient for robustness:

$$\eta_i(\mathbf{x}) = \frac{1}{K} \sum_{\mathbf{x}_j \in N(\mathbf{x}_i)} \hat{g}_j(\mathbf{x}), \quad \mathbf{x} \in \mathbb{R}^3, \quad (5)$$

where $kN(\mathbf{x}_i)$ is the k -nearest neighborhood of \mathbf{x}_i .

Finally, we propose to perform point cloud denoising by updating point coordinates with momentum gradient ascent:

$$\begin{aligned} \gamma_i^{(0)} &= \mathbf{0} \in \mathbb{R}^3, \\ \mathbf{x}_i^{(0)} &= \mathbf{x}_i, \quad \mathbf{x}_i \in \mathbf{X}, \\ \gamma_i^{(t)} &= \alpha^{(t)} \eta_i(\mathbf{x}_i^{(t-1)}) + (1 - \alpha^{(t)}) \gamma_i^{(t-1)}, \\ \mathbf{x}_i^{(t)} &= \mathbf{x}_i^{(t-1)} + \beta^{(t)} \gamma_i^{(t)}, \quad t = 1, \dots, T, \end{aligned} \quad (6)$$

where t is the iterative step, $\alpha^{(t)}$ is the momentum weight, $\beta^{(t)}$ is the step size. While Score requires a sufficient number of total steps $T = 30$ to ensure optimal performance, our method applies momentum gradient ascent, thus reducing the step number to $T = 15$ while achieving better performance.

Moreover, as Figure 3 shows, compared to classical gradient ascent used in Score, momentum gradient ascent leverages the information of previous iterations in determining the trajectories of points, thereby benefiting solution stability and inference time.

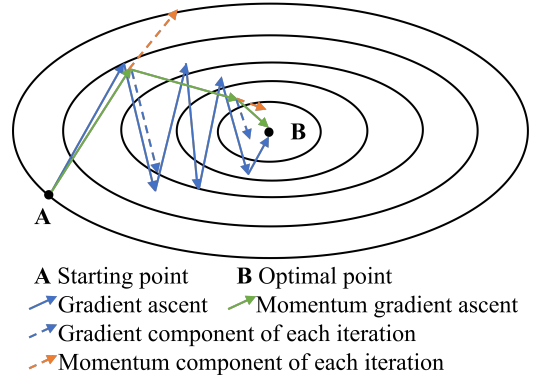


Fig. 3: Comparison of classical gradient ascent and momentum gradient ascent.

4. EXPERIMENT

4.1. Experimental Setting

Dataset. We adopt 20 meshes from the commonly used PU-Net dataset [15] for training, and 20 meshes for testing, with the sampling resolutions ranging from 10K to 50K points. The point clouds are normalized to the unit sphere, and perturbed by Gaussian noise with standard deviation from 1% to 3% of the radius of the bounding sphere. Similar to previous works [10, 13], point clouds are split into patches as input.

Baselines. One traditional optimization-based method, bilateral filtering [14], and three state-of-the-art deep-learning-based approaches including PCNet [10], DMR [13] and Score [11] are used for comparison.

Metric. Two commonly used metrics are adopted for quantitative evaluation, the Chamfer distance (CD) [16] and point-to-mesh distance (P2M) [17].

4.2. Quantitative and Qualitative Results

As Table 1 shows, our model significantly outperforms previous methods bilateral filtering [14], PCNet [10], DMR [13], and surpasses Score [11] in the majority of cases.

To further illustrate the effectiveness of our method, we compare the qualitative performance with the competitive baseline Score [11]. As Figure 4 shows, compared to

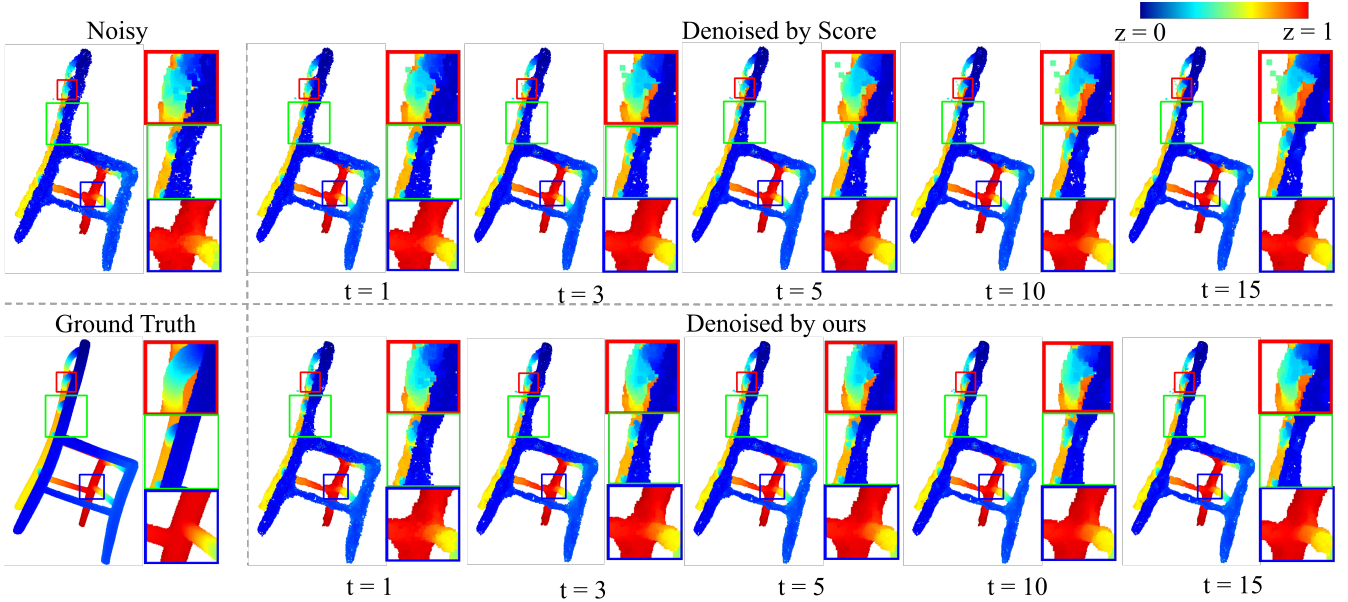


Fig. 4: Point cloud denoising comparisons on the dense point cloud `chair` of the PU-Net dataset [15]. The color of each 3D point varies according to its z coordinate (perpendicular to the plane).

# Points	10K (Sparse)	50K (Dense)
Score [11]	0.66	6.27
Ours	0.40	4.76

Table 2: Average inference time per point cloud in minutes on PU-Net [15] dataset using identical environments.

Score [11], our denoised point clouds feature fewer outliers, better structures and smoother outlines in all the iterative steps. In Figure 5, Score takes 30 steps to achieve optimal denoising results, while ours takes only 15 steps and outputs results with fewer outliers and smoother outlines.

4.3. Inference Time

As Table 2 shows, Score requires longer inference time. Unlike gradient ascent in Score, momentum gradient ascent utilizes previous iterations to seek promising directions to move forward, thus saving inference time by reducing iterations.

5. CONCLUSION

In this paper, we propose point cloud denoising via momentum ascent in gradient fields. To improve the previous gradient-based method, we leverage the information of previous iterations in determining the trajectories of points, thus benefiting the solution stability and inference time. Experiments demonstrate that our method outperforms state-of-the-art methods with a variety of point clouds and noise levels.

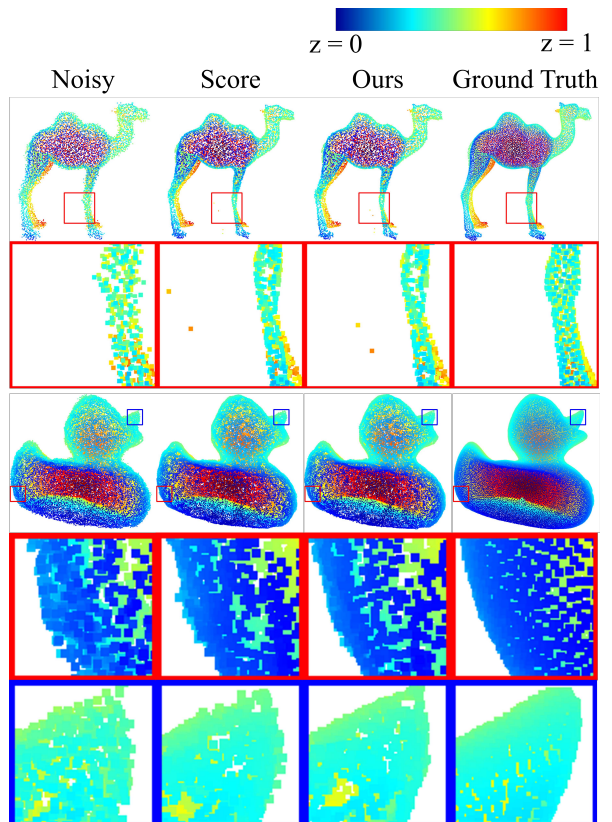


Fig. 5: Point cloud denoising comparisons on the sparse point cloud `camel` and the dense point cloud `duck` of the PU-Net dataset [15]. The color of each 3D point varies according to its z coordinate (perpendicular to the plane).

6. REFERENCES

- [1] Marc Alexa, Johannes Behr, Daniel Cohen-Or, Shachar Fleishman, David Levin, and Claudio T Silva, "Point set surfaces," in *Proceedings Visualization, 2001. VIS'01.* IEEE, 2001, pp. 21–29.
- [2] Haim Avron, Andrei Sharf, Chen Greif, and Daniel Cohen-Or, "11-sparse reconstruction of sharp point set surfaces," *ACM Transactions on Graphics (TOG)*, vol. 29, no. 5, pp. 1–12, 2010.
- [3] Frédéric Cazals and Marc Pouget, "Estimating differential quantities using polynomial fitting of osculating jets," *Computer Aided Geometric Design*, vol. 22, no. 2, pp. 121–146, 2005.
- [4] Hui Huang, Shihao Wu, Minglun Gong, Daniel Cohen-Or, Uri Ascher, and Hao Zhang, "Edge-aware point set resampling," *ACM transactions on graphics (TOG)*, vol. 32, no. 1, pp. 1–12, 2013.
- [5] Enrico Mattei and Alexey Castrodad, "Point cloud denoising via moving rpca," in *Computer Graphics Forum*. Wiley Online Library, 2017, vol. 36, pp. 123–137.
- [6] Yujing Sun, Scott Schaefer, and Wenping Wang, "Denoising point sets via l0 minimization," *Computer Aided Geometric Design*, vol. 35, pp. 2–15, 2015.
- [7] Chaojing Duan, Siheng Chen, and Jelena Kovacevic, "3d point cloud denoising via deep neural network based local surface estimation," in *ICASSP 2019-2019 IEEE International Conference on Acoustics, Speech and Signal Processing (ICASSP)*. IEEE, 2019, pp. 8553–8557.
- [8] Pedro Hermosilla, Tobias Ritschel, and Timo Ropinski, "Total denoising: Unsupervised learning of 3d point cloud cleaning," in *Proceedings of the IEEE/CVF International Conference on Computer Vision*, 2019, pp. 52–60.
- [9] Francesca Pistilli, Giulia Fracastoro, Diego Valsesia, and Enrico Magli, "Learning graph-convolutional representations for point cloud denoising," in *European conference on computer vision*. Springer, 2020, pp. 103–118.
- [10] Marie-Julie Rakotosaona, Vittorio La Barbera, Paul Guerrero, Niloy J Mitra, and Maks Ovsjanikov, "Pointcleannet: Learning to denoise and remove outliers from dense point clouds," in *Computer Graphics Forum*. Wiley Online Library, 2020, vol. 39, pp. 185–203.
- [11] Shitong Luo and Wei Hu, "Score-based point cloud denoising," in *Proceedings of the IEEE/CVF International Conference on Computer Vision*, 2021, pp. 4583–4592.
- [12] Boris T Polyak, "Some methods of speeding up the convergence of iteration methods," *Ussr computational mathematics and mathematical physics*, vol. 4, no. 5, pp. 1–17, 1964.
- [13] Shitong Luo and Wei Hu, "Differentiable manifold reconstruction for point cloud denoising," in *Proceedings of the 28th ACM international conference on multimedia*, 2020, pp. 1330–1338.
- [14] Julie Digne and Carlo De Franchis, "The bilateral filter for point clouds," *Image Processing On Line*, vol. 7, pp. 278–287, 2017.
- [15] Lequan Yu, Xianzhi Li, Chi-Wing Fu, Daniel Cohen-Or, and Pheng-Ann Heng, "Pu-net: Point cloud upsampling network," in *Proceedings of the IEEE conference on computer vision and pattern recognition*, 2018, pp. 2790–2799.
- [16] Haoqiang Fan, Hao Su, and Leonidas J Guibas, "A point set generation network for 3d object reconstruction from a single image," in *Proceedings of the IEEE conference on computer vision and pattern recognition*, 2017, pp. 605–613.
- [17] Nikhila Ravi, Jeremy Reizenstein, David Novotny, Taylor Gordon, Wan-Yen Lo, Justin Johnson, and Georgia Gkioxari, "Accelerating 3d deep learning with pytorch3d," *arXiv preprint arXiv:2007.08501*, 2020.